The AAPS Journal (2019) 21: 20
DOI: 10.1208/s12248-019-0294-1

Research Article

Quantitative Prediction of Human Hepatic Clearance for P450 and Non-P450 Substrates from *In Vivo* Monkey Pharmacokinetics Study and *In Vitro* Metabolic Stability Tests Using Hepatocytes

Haruka Nishimuta,[1,2] Takao Watanabe,[1] and Kiyoko Bando[1]

Received 3 July 2018; accepted 2 January 2019; published online 23 January 2019

Abstract. Accurate prediction of human pharmacokinetics for drugs remains challenging, especially for non-cytochrome P450 (P450) substrates. Hepatocytes might be suitable for predicting hepatic intrinsic clearance (CL_{int}) of new chemical entities, because they can be applied to various compounds regardless of the metabolic enzymes. However, it was reported that hepatic CL_{int} is underestimated in hepatocytes. The purpose of the present study was to confirm the predictability of human hepatic clearance for P450 and non-P450 substrates in hepatocytes and the utility of animal scaling factors for the prediction using hepatocytes. CL_{int} values for 30 substrates of P450, UDP-glucuronosyltransferase, flavin-containing monooxygenase, esterases, reductases, and aldehyde oxidase in human microsomes, human S9 and human, rat, and monkey hepatocytes were estimated. Hepatocytes were incubated in serum of each species. Furthermore, CL_{int} values in human hepatocytes were corrected with empirical, monkey, and rat scaling factors. CL_{int} values in hepatocytes for most compounds were underestimated compared to observed values regardless of the metabolic enzyme, and the predictability was improved by using the scaling factors. The prediction using human hepatocytes corrected with monkey scaling factor showed the highest predictability for both P450 and non-P450 substrates among the predictions using liver microsomes, liver S9, and hepatocytes with or without scaling factors. CL_{int} values by this method for 80% and 90% of all compounds were within 2- and 3-fold of observed values, respectively. This method is accurate and useful for estimating new chemical entities, with no need to care about cofactors, localization of metabolic enzymes, or protein binding in plasma and incubation mixture.

KEY WORDS: hepatic clearance; *in vitro-in vivo* extrapolation; monkey; non-P450; P450.

INTRODUCTION

Accurate prediction of human pharmacokinetics is very important in the selection of candidates in drug discovery and reduction of the dropout rate in drug development. Hepatic clearance is the most significant elimination pathway and an important pharmacokinetic parameter that is involved in half-life and oral bioavailability. The elimination pathway of approximately 70% of marketed drugs is metabolism in liver (1–3).

Various methods have been developed to predict human hepatic clearance using *in vivo* and/or *in vitro* data. Empirical methods using *in vivo* data, such as allometric scaling from pre-clinical species, have been widely used (4,5). However, the predictability of this method is questionable, because most metabolic enzymes have large species differences (6). Since the emergence of commercial human liver materials such as liver microsomes and cryopreserved hepatocytes, a physiologically based *in vitro-in vivo* extrapolation (IVIVE) method has been developed (7,8). It was reported that this IVIVE method using liver microsomes and cryopreserved hepatocytes tends to under-predict human hepatic intrinsic clearance (CL_{int}) (9). Although various other methods are reported, which method is the most suitable for predicting human hepatic clearance (CL_h) remains uncertain.

Recently, pharmaceutical industries in drug discovery have conducted metabolic stability tests using human liver microsomes with NADPH to remove compounds that have high clearances. Our knowledge of methods to design drugs that are hardly metabolized by P450 has increased. Microsomes with NADPH system cannot estimate the compounds that are metabolized by cytosolic enzymes or enzymes that

Electronic supplementary material The online version of this article (https://doi.org/10.1208/s12248-019-0294-1) contains supplementary material, which is available to authorized users.

[1] Preclinical Research Unit, Sumitomo Dainippon Pharma Co., Ltd., 3-1-98 Kasugade-naka, Konohana-ku, Osaka, 554-0022, Japan.
[2] To whom correspondence should be addressed. (e–mail: haruka-nishimuta@ds-pharma.co.jp)

need cofactors other than NADPH. Consequently, the number of drug candidates that are metabolized by non-P450 enzymes has risen. However, the accurate prediction of *in vivo* CL_h based on *in vitro* CL_{int} is still challenging, especially for substrates of non-P450 enzymes (10). Several non-P450 enzymes are expressed in the cytosolic fraction. Liver S9 fraction would be a useful tool to estimate total metabolic activity of P450 and non-P450 enzymes, although it is necessary to add appropriate cofactors in the incubation. However, the prediction of CL_{int} using S9 has been scarcely reported so far.

Hepatocytes might be more suitable for predicting CL_{int} of new chemical entities compared with microsomes and S9, because they can be applied to various kinds of compounds regardless of cofactors and localization of metabolic enzymes. In the IVIVE method, it is necessary to correct the CL_{int} in microsomes, S9, and hepatocytes with nonspecific binding in the incubation mixture (11,12). In addition, in this method the fraction unbound in human plasma ($f_{u,p}$) is needed to calculate CL_h based on CL_{int}. Obtaining these parameters is troublesome and causes inaccurate predictions, because quite a few compounds show nonspecific binding to the apparatus and equilibrium is sometimes not fully achieved in the equilibrium dialysis assay (13). Shibata *et al.* reported a "serum incubation method" using cryopreserved hepatocytes (14–16). This method uses serum instead of medium and does not require consideration of $f_{u,p}$ or the fraction unbound in the incubation mixture ($f_{u,inc}$). However, human hepatic CL_{int} was underestimated by this method as well as the method using medium.

Naritomi *et al.* reported that successful predictions of human hepatic clearance (mostly within 2-fold of the actual values) were obtained for P450 substrates by use of the human $CL_{int,in\ vitro}$ in microsomes corrected with rat or dog scaling factors, which are the ratios of $CL_{int,in\ vivo}$ to $CL_{int,in\ vitro}$ (17). They also reported that the prediction using hepatocytes corrected with rat scaling factor showed low predictability (only 1 out of 8 compounds was within 2-fold of the actual values), although the scaling factors improved the predictability in comparison with the case of no scaling factor (18). However, there has been no report about the prediction using hepatocytes and monkey scaling factor.

The purpose of the present study was to confirm the predictability of human hepatic clearance for P450 and non-P450 substrates in hepatocytes and the utility of animal scaling factors for the prediction using hepatocytes. Predictability of the prediction methods using microsomes, S9, cryopreserved hepatocytes with or without scaling factor for substrates of P450, UDP-glucuronosyltransferase (UGT), flavin-containing monooxygenase (FMO), esterases, reductases, and aldehyde oxidase (AO) was evaluated (Supplemental Table 1). The metabolic stabilities in human microsomes with NADPH and cofactor of each enzyme, human S9 with NADPH and cofactor of each enzyme, and human, rat, and monkey hepatocytes with serum of each animal were estimated and CL_{int} values in these systems were calculated. Furthermore, CL_{int} values in human hepatocytes corrected with empirical, monkey, and rat scaling factors were investigated. The CL_{int} values estimated by these methods were compared with observed CL_{int} values in humans.

MATERIALS AND METHODS

Chemicals

Alprenolol hydrochloride, (R)-atomoxetine hydrochloride, desipramine hydrochloride, diclofenac sodium salt, haloperidol, imipramine hydrochloride, lansoprazole, mycophenolic acid, paroxetine maleate, ranitidine hydrochloride, rivastigmine tartrate, carbamazepine, cisapride monohydrate, nicardipine hydrochloride, nimodipine, telmisartan, zaleplon, zoniporide hydrochloride hydrate, and flecainide acetate were purchased from Sigma-Aldrich Co. (St. Louis, MO); clozapine, gemfibrozil, ketanserin tartrate, paclitaxel, omeprazole, mebendazole, midazolam, and nifedipine from Wako Pure Chemical Industries Ltd. (Osaka, Japan); felodipine from LKT Laboratories (St. Paul, MN); flumazenil from Enzo Life Sciences, Inc. (Farmingdale, NY); oxybutynin chloride and ziprasidone hydrochloride monohydrate from Toronto Research Chemicals (North York, ON, Canada); and β-NADPH and β-NADH from Oriental Yeast Co., Ltd. (Tokyo, Japan). All other reagents and solvents were of analytical grade.

Microsomes, S9, Hepatocytes, and Serum

Human liver microsomes (mixed gender; pool of 200), human liver S9 (mixed gender; pool of 50), and cryopreserved human (mixed gender; pool of 20), cynomolgus monkey (male; pool of 3), and Sprague Dawley (SD) rat (male; pool of 8) hepatocytes were purchased from Xenotech, LLC (Lenexa, KS). Pooled human cryopreserved hepatocytes were prepared using a single-freeze process (CryostaX™). Pooled human serum was purchased from Cosmo Bio Co., Ltd. (Tokyo, Japan). Pooled cynomolgus monkey and SD rat sera were purchased from Valley Biomedical Products & Services, Inc. (Winchester, VA).

Animals

Male cynomolgus monkeys, 2–4 years old, were supplied by Guangxi Xiongsen Experimental Primate Animals Breeding and Developing Limited Company (Guangxi, China) and bred in a temperature- and humidity-controlled room with 12 h light/dark cycle. They were fed commercial monkey diet and fasted overnight prior to drug administration, with *ad libitum* access to water. All procedures were approved by the Sumitomo Dainippon Pharmaceutical Committee on Animal Research.

Male SD rats, 7 weeks old, were supplied by Charles River Laboratories Japan, Inc. (Kanagawa, Japan) and bred in a temperature- and humidity-controlled room with 12 h light/dark cycle. They were fed commercial rodent diet and fasted overnight prior to drug administration, with *ad libitum* access to water. All procedures were approved by the Sumitomo Dainippon Pharmaceutical Committee on Animal Research.

Metabolic Stabilities in Microsomes and S9 for P450 Substrates, Reductase Substrates, AO Substrates, FMO Substrates, and Esterase Substrates

Substrates (final concentration, 200 nM) were incubated at 37°C in 100 μL of a reaction mixture consisting of 50 mM phosphate buffer (pH 7.4), cofactors (3 mM β-NADPH and 3 mM β-NADH for reductase substrates and 3 mM β-NADPH for other substrates), and subcellular fractions (microsomes and S9 from humans). Linearity of metabolic activities for concentrations of subcellular fractions and incubation times (5, 15, 30, or 60 min) were confirmed, and the optimal conditions were set for each compound (Supplemental Table 2). The final concentration of acetonitrile in the reaction mixture was 0.5% (*v*/*v*). After warming at 37°C for 5 min, the reactions were initiated by the addition of NADPH for P450 substrates or the substrates for other compounds and stopped by addition of 200 μL of ice-cold acetonitrile for esterase substrates or ice-cold methanol for other compounds. Control samples were incubated using the same method in the absence of NADPH or substrates; the NADPH or substrates were added after addition of ice-cold acetonitrile or methanol. The reaction mixtures were mixed with 200 μL acetonitrile containing 200 nM flecainide (internal standard) for esterase substrates or methanol containing the internal standard for other compounds. The mixtures were centrifuged at 4500 rpm for 10 min. The supernatants were filtered through 96-well filter plates with 0.45-μm pore size (Varian Inc., Palo Alto, CA, USA). The filtrates were diluted 2-fold with distilled water and transferred to 96-well plates. A 10-μL portion was then injected into a high-performance liquid chromatography-tandem mass spectrometry (HPLC-MS/MS) system.

Metabolic Stabilities in Microsomes and S9 for UGT Substrates

Incubation was performed in accordance with previous reports with some exceptions (19,20). UGT substrates (final concentration: 200 nM) were incubated at 37°C in 100 μL of a reaction mixture consisting of 50 mM phosphate buffer (pH 7.4), human microsomes or S9, 3.4 mM magnesium chloride, 1.15 mM EDTA, 115 μM saccharic acid lactone, 5 mM UDPGA, 3 mM NADPH, and 2% BSA. Microsomes or S9 were activated in advance by addition of 10 μg alamethicin/mg microsomal or S9 protein and put on ice for 15 min. Linearity of metabolic activities for concentrations of subcellular fractions and incubation times (15, 60, or 120 min) were confirmed, and the optimal reaction conditions were set for each compound (Supplemental Table 2). The final concentration of organic solvent in the incubation mixture was 0.5% (*v*/*v*). After warming at 37°C for 5 min, the reaction was then initiated by the addition of a mixed cofactor solution containing UDPGA and NADPH and stopped by addition of 200 μL of ice-cold methanol. Control samples were incubated using the same method in the absence of the mixed cofactor solution and added to the mixed cofactor solution after addition of ice-cold methanol. The reaction mixtures were spiked with 200 μL of methanol containing the internal standard, 200 nM flecainide, and centrifuged at 4500 rpm for 10 min. The supernatants were filtered using 0.45-μm 96-well filter plates (Varian, Inc., Palo Alto, CA). The filtrates were then diluted 2-fold with distilled water and transferred to 96-well plates. A 10-μL portion was injected into an HPLC-MS/MS system.

The Fraction Unbound in Incubations

The unbound fractions in incubation mixture ($f_{u,inc}$) were determined using a dialysis plate, for which a 96-well equilibrium dialyzer (10-kDa molecular mass cutoff) was purchased from Harvard Apparatus (Holliston, MA, USA); 50 mM phosphate buffer (150 μL, pH 7.4) containing compounds (1 μM, final) and subcellular fractions (microsomes and S9) were respectively added to the acceptor chambers. In addition, 2% BSA was added for UGT substrates; 50 mM phosphate buffer (150 μL, pH 7.4) was added to the donor chambers. The dialysis plate on a plate rotator was put in an incubator at 37°C for 22 h. Samples (30 μL) from the acceptor chambers were mixed with 30 μL of 50 mM phosphate buffer (pH 7.4), and 30 μL of samples from the donor chambers were mixed with 30 μL of subcellular fractions (and 2% BSA for UGT substrates) in 50 mM phosphate buffer (pH 7.4). These samples were then mixed with 200 nM flecainide (internal standard) in 240 μL of methanol (or acetonitrile for esterase substrates) and centrifuged at 4500 rpm for 10 min. The supernatants were filtered through 0.45-μm 96-well filter plates (Varian, Inc., Palo Alto, CA, USA). The filtrates were then diluted 2-fold with distilled water and transferred to 96-well plates. A 10-μL portion was injected into an HPLC-MS/MS system.

Metabolic Stabilities in Human, Monkey, and Rat Hepatocytes

Cryopreserved monkey and rat hepatocytes were thawed in a water bath at 37°C for 1.5 min. Cryopreserved human hepatocytes were not thawed in the vial in accordance with protocol, because they were of tablet form and could be taken from the vial without prior thawing. The hepatocytes were added into pre-warmed tube A (supplemented Dulbecco's modified Eagle's medium and isotonic Percoll) of a hepatocyte isolation kit (XenoTech LLC) and then centrifuged at 740 rpm for 5 min at 25°C. The supernatant was removed and the pellet was suspended with 5 mL of pre-warmed Tube B solution (supplemented Dulbecco's modified Eagle's medium) of the hepatocyte isolation kit. The number of viable cells was counted using trypan blue and the viability was confirmed to be > 85%. The remaining medium from tube B was added into the cell suspension and suspended. The suspension was centrifuged at 550 rpm for 3 min at 25°C. After removal of the supernatant, the cells were suspended in human, monkey, or rat serum and 75 μL of the suspension was distributed in 96-well plates. Linearity of metabolic activities for density of hepatocytes and incubation times (15, 60, or 120 min) were confirmed, and the optimal reaction conditions were set for each compound (Supplemental Table 2). After pre-incubation of the hepatocyte suspensions in CO_2 incubator under 5% CO_2 at 37°C for 5 min, the reactions were initiated by the addition of 75 μL of 400 nM substrates in the serum and stopped by taking 25 μL samples. Samples were taken at 0, 15, 60, or 120 min time points. The final concentration of acetonitrile in the incubation mixture was 0.1% (*v*/*v*). The samples were immediately added into 200 nM flecainide (internal standard) in 200 μL of ice-cold methanol (or ice-cold acetonitrile for esterase substrates). These samples were mixed and then centrifuged at 4500 rpm for 10 min. The supernatants were then filtered using 0.45-μm 96-well filter plates and diluted 2-fold with distilled water for HPLC-MS/MS.

Pharmacokinetic Study in Monkeys

Compounds were dissolved in saline containing 0–50% (*v*/*v*) polyethylene glycol 400, and the i.v. dosing solutions (0.1–1 mg/1–2 mL/kg) were administered to three or four male cynomolgus monkeys. Administration was conducted with a washout period of at least 6 days. Blood samples were collected from the antebrachial vein at appropriate times and centrifuged at 6000 rpm for 15 min at 4°C. The supernatants were obtained as plasma samples. Urine samples were collected for 24 h using collection trays and the volume was measured. The plasma and urine samples were kept at − 20°C until analysis.

Pharmacokinetic Study in Rats

Compounds were dissolved in saline containing 0–50% (*v*/*v*) polyethylene glycol 400, and the i.v. dosing solutions (0.1–0.5 mg/1–5 mL/kg) were administered to three male SD rats. Blood samples were collected from the jugular vein at appropriate times and centrifuged at 3000 rpm for 10 min at 4°C. The supernatants were obtained as plasma samples. Urine samples were collected for 24 h using collection trays and the volume was measured. The plasma and urine samples were kept at − 20°C until analysis.

Measurement of Concentration in Monkey and Rat Plasma and Urine

Plasma or urine (50 μL) and 600 μL of 200 nM flecainide (internal standard) in ethyl acetate were mixed well, then centrifuged at 4500 rpm for 5 min. The supernatants were evaporated and the residues were dissolved in 200 μL of 50% (*v*/*v*) acetonitrile in distilled water for esterase substrates or 50% (*v*/*v*) methanol in distilled water for other compounds. The supernatants were then filtered using 0.45-μm 96-well filter plates and diluted 2-fold with distilled water for HPLC-MS/MS.

Concentration Ratio in Rat Blood Plasma

Blood was collected from two rats using heparin and the two samples were pooled. The blood samples containing compounds (100 nM) were put in an incubator at 37°C for 10 min. The blood samples were then centrifuged at 4500 rpm for 10 min and the supernatants were obtained as plasma samples. Blank plasma was obtained by centrifugation of the blood in the same way. The blank plasma samples containing compounds (100 nM) were prepared as standard samples. The incubated samples or the standard samples (50 μL) were mixed with 200 μL of ice-cold methanol (or ice-cold acetonitrile for esterase substrates) containing the internal standard, 200 nM flecainide. These samples were centrifuged at 4500 rpm for 10 min. The supernatants were then filtered using 0.45-μm 96-well filter plates and diluted 2-fold with distilled water for HPLC-MS/MS.

Analytical Procedures

Concentrations of compounds in samples were measured using an HPLC-MS/MS system consisting of a TSQ 7000 mass spectrometer (Thermo Fisher Scientific Inc., Waltham, MA, USA) with a Shimadzu 10A series HPLC system (Shimadzu Corporation, Kyoto, Japan); or a TSQ Quantum Ultra mass spectrometer (Thermo Fisher Scientific Inc.) with a Shimadzu 20A series HPLC system (Shimadzu Corporation); or an API4000 *mass* spectrometer (Applied Biosystems, Forester City, CA, USA) with a Shimadzu 10A series HPLC system; or an API3200QTrap mass spectrometer (Applied Biosystems) with a Shimadzu 20A series HPLC system. The analytical conditions of HPLC are shown in Supplemental Table 1. Mass spectrometric detection was conducted by positive or negative ionization electrospray. The selective reaction monitoring mode was used as follows to monitor ions (*m*/*z*: precursor ion → product ion): lansoprazole (370.1 → 252.1), omeprazole (346.1 → 198.2), paclitaxel (854.4 → 286.0), alprenolol (250.0 → 116.0), atomoxetine (256.1 → 148.2), desipramine (267.1 → 72.1), imipramine (281.1 → 86.1), paroxetine (330.0 → 192.0), carbamazepine (237.0 → 194.0), cisapride (467.1 → 183.9), felodipine (384.0 → 337.9), midazolam (326.0 → 291.0), nicardipine (480.2 → 315.1), nifedipine (347.0 → 254.0), nimodipine (419.2 → 343.1), diclofenac (293.9 → 249.9), gemfibrozil (249.2 → 120.9), mycophenolic acid (319.1 → 191.1), telmisartan (515.2 → 276.2), haloperidol (375.7 → 164.9), ketanserin (396.0 → 188.8), mebendazole (295.8 → 263.8), zaleplon (306.1 → 235.6), ziprasidone (413.1 → 193.6), zoniporide (320.9 → 262.3), clozapine (326.8 → 269.9), ranitidine (315.2 → 176.1), flumazenil (303.8 → 257.5), oxybutynin (358.2 → 124.1), rivastigmine (315.2 → 176.1), and flecainide (415.1 → 398.1 for positive ion mode or 412.9 → 270.0 for negative ion mode).

Data Analysis

The peak area ratios of compounds to internal standard were used for all of the calculations in this study. For metabolic stability studies, three determinations *versus* incubation time were plotted on a semi-logarithmic scale, and the mean value of the slopes was calculated by linear regression analysis as the elimination rate constant (k_{el} (min^{-1})). For low turnover compounds, remaining ratio < 90% data were used for CL_{int} calculation. Examples of depletion time profiles in human hepatocytes incubations are shown in Supplemental Fig. 1. The unbound intrinsic clearance values were calculated using Eq. 1 for human microsomes and S9 and Eq. 2 for human, monkey, and rat hepatocytes (Supplemental Table 3). The $f_{u,inc}$ values were not assigned for hepatocytes, because serum incubation method was used in this study.

$$CL_{int}\ (\mathrm{mL/min/mg\ protein}) = \frac{k_{el}\ (\mathrm{min^{-1}})}{\text{microsomal or S9 concentration (mg protein/mL)}} \times \frac{1}{f_{u,inc}} \quad (1)$$

$$CL_{int}\ (\mathrm{mL/min/10^6\ cells}) = \frac{k_{el}\ (\mathrm{min^{-1}})}{\text{hepatocytes concentration } (10^6\ \text{cells/mL})} \quad (2)$$

The $f_{u,inc}$ values in human microsomes and S9 were investigated using Eq. 3, and the mean of three determinations was calculated. It was assumed that the $f_{u,inc}$ values in animal subcellular fractions were equivalent to those in human subcellular fractions. It was reported that species differences in $f_{u,inc}$ of liver microsomes were less than 2-fold for most of 43 drugs (21). In case of necessity, the $f_{u,inc}$ value for each

subcellular concentration was estimated by Langmuir equation assuming that the protein binding concentration was proportional to the free concentration (22).

$$f_{u,inc} = \frac{\text{peak area in buffer sample/peak area of internal standard}}{\text{peak area in microsomal or S9 sample/peak area of internal standard}} \quad (3)$$

The $CL_{int,\ in\ vitro}$ values were calculated using Eq. 4 for human microsomes and S9 or Eq. 5 for human, monkey, and rat hepatocytes using physiological parameters (Table I) (23,24). The $f_{u,p}$ values were not assigned for hepatocytes, because serum incubation method was used in this study.

$$CL_{int,invitro}\ (\text{mL/min/kg}) = CL_{int}\ (\text{mL/min/mg protein}) \times \frac{\text{Microsomal or S9 protein/Liver weight} \times \text{Liver weight} \times f_{u,p}/R_b}{\text{Body weight}} \quad (4)$$

$$CL_{int,invitro}\ (\text{mL/min/kg}) = CL_{int}\ (\text{mL/min/}10^6\ \text{cells}) \times \frac{\text{Hepatocytes/Liver weight} \times \text{Liver weight}/R_b}{\text{Body weight}} \quad (5)$$

where $f_{u,p}$ represents unbound fraction in plasma (Supplemental Table 4) and R_b represents blood-to-plasma concentration ratio. These $CL_{int,\ in\ vitro}$ values were used as $CL_{int,\ predicted}$ values for prediction without scaling factor.

Investigated rat R_b values were calculated using Eq. 6, and the mean of three determinations was calculated. Reported R_b values were used as human R_b values. In the case of lack of reported data, these investigated rat R_b values were used. Monkey R_b values were assumed to be the same as the values used as human R_b values (Supplemental Table 4).

$$R_b = \frac{\text{peak area of test compound in standard sample/peak area of internal standard in standard sample}}{\text{peak area of test compound in test sample/peak area of internal standard in test sample}} \quad (6)$$

Calculation of $CL_{int,observed}$

Human $CL_{int,observed}$ values were calculated from Eqs. 7–10 using a dispersion model (25). We selected the dispersion model because it was reported that the model showed good predictability of hepatic availability not only for low clearance drugs, but also for high clearance drugs (8). The blood protein binding values were not assigned in Eq. 9, because the human $CL_{int,observed}$ values were compared with the $CL_{int,predicted}$ values estimated by the serum incubation method for hepatocytes.

$$F_h = \frac{4a}{(1+a)^2\exp[(a-1)/2D_N] - (1-a)^2\exp[-(a+1)/2D_N]} \quad (7)$$

$$a = (1 + 4R_N \times D_N)^{1/2} \quad (8)$$

$$R_N = CL_{int}/Q_h \quad (9)$$

$$D_N = 0.17 \quad (10)$$

where Q_h (mL/min/kg) represents liver blood flow and F_h represents the hepatic availability. F_h values were calculated from Eqs. 11 and 12 assuming that all of the non-renal clearance is hepatic clearance.

$$CL_h = \frac{CL_{total,p}}{R_b} \times \left(100 - \frac{f_e}{100}\right) \quad (11)$$

$$F_h = 1 - \frac{CL_h}{Q_h} \quad (12)$$

where $CL_{total,p}$ (mL/min/kg) represents total clearance in plasma after intravenous administration, and f_e (%) represents the fraction of the dose excreted in urine as unchanged drug. The reported values were used for humans (Supplemental Table 4).

Estimation of Scaling Factors from Monkey and Rat Plasma Concentrations

Pharmacokinetic parameters in monkeys and rats were calculated for individual animals by noncompartmental analysis. The area under the plasma concentration-time curve extrapolated to infinity (AUC_{inf}) and total clearance in plasma ($CL_{total,p}$) were calculated as follows:

$$AUC_{inf} = AUC_t + \frac{C_t}{k} \quad (13)$$

$$CL_{total,p} = \frac{D}{AUC_{inf}} \quad (14)$$

where AUC_t represents the area under the curve from time zero to the time of the last measurable concentration; C_t represents the plasma concentration at the corresponding time, calculated with use of the regression equation for estimation of the elimination rate constant; k represents the terminal rate constant determined by logarithmic regression analysis; and D represents dose.

Table I. Physiological Parameters for Prediction of CL_{int} in Humans, Monkeys, and Rats

	Body weight kg	Liver weight g	Microsomal protein per liver weight mg/g	S9 protein per liver weight mg/g	Hepatocytes per liver weight 10^6 cells/g	Liver blood flow mL/min/kg
Human	70[a]	1470[a]	45[a]	120.7[b]	120[a]	20[a]
Monkey	3.5[a]	112[a]	–	–	120[a]	44[a]
Rat	0.25[a]	10[a]	–	–	135[a]	70[a]

[a] Hosea *et al.*, 2009
[b] Houston and Galetin, 2008

$CL_{int,in\ vivo}$ values for monkeys and rats, as well as for humans, were calculated from Eqs. 7–12 using dispersion model. The f_e values for monkeys and rats were calculated using Eq. 15.

$$f_e = \frac{C_{urine} \times V_{urine}}{D} \times 100 \quad (15)$$

where D (mg) represents dose, C_{urine} (mg/mL) represents the urine concentration, and V_{urine} (mL) represents the volume of urine.

Scaling factors in monkey or rat were calculated from Eq. 16 for each compound. The calculated scaling factor values are shown in Supplemental Table 4. Each scaling factor was applied to each compound.

$$\text{Scaling factor} = \frac{CL_{int,\ invivo}}{CL_{int,\ invitro}} \quad (16)$$

Prediction of Human CL_{int}

$CL_{int,predicted}$ values for humans from microsomes, S9, and hepatocytes without scaling factors were the $CL_{int,predicted}$ values calculated from Eqs. 4 and 5. $CL_{int,predicted}$ values for humans from hepatocytes corrected with empirical, monkey, and rat scaling factors were calculated from Eq. 17. The empirical scaling factor was set as "3.1," which was calculated from a fitting line (linear regression, slope = 1) for log-log plots of $CL_{int,observed}$ *versus* $CL_{int,hepatocytes}$ for 30 compounds investigated in this study ($y = x - 0.489$).

$$CL_{int,\ predicted} = CL_{int,\ invitro} \times \text{Scaling factor} \quad (17)$$

Statistical Analysis

The prediction accuracies were estimated by average fold error (AFE) (Eq. 18) (26).

$$AFE = 10^{\left|\frac{\sum \log\left(\frac{observed}{predicted}\right)}{N}\right|} \quad (18)$$

The predictabilities for substrates of each enzyme and all compounds were estimated by "a ratio of compounds whose predicted values were within 3-fold of observed values," and combination of "a ratio of compounds whose predicted values were within 3-fold of observed values" and "a reduction in AFE," respectively.

RESULTS

Correlations among Predicted CL_{int} Values from Human Microsomes, S9, and Hepatocytes

Relationships among $CL_{int,predicted}$ values from human microsomes, S9, and hepatocytes are shown in Table II and Fig. 1. For P450 substrates, microsomes and S9 showed comparable CL_{int} values. CL_{int} values in microsomes and S9 for most P450 and UGT substrates were higher than those in human hepatocytes. On the other hand, CL_{int} values in microsomes for most AO and esterase substrates were much lower than those in S9 and hepatocytes. Far from the values in microsomes, S9 showed comparable CL_{int} values (within 3-fold) with human hepatocytes for 8 out of 9 compounds of reductase, AO, and esterase substrates. CL_{int} values in microsomes, S9, and hepatocytes for all of the FMO substrates were comparable (within 2-fold).

Prediction of Hepatic CL_{int} Using Metabolic Stability in Human Microsomes, S9, and Hepatocytes

Predictability of CL_{int} values using metabolic stability in human microsomes, S9, and hepatocytes is shown in Tables II and III and Fig. 2. In microsomes, CL_{int} values for 10/15 (number of drugs/total drugs) of P450 substrates, 1/4 of UGT substrates, and 2/2 of FMO substrates were predicted within 3-fold of observed values. In S9, CL_{int} values for 9/15 of P450 substrates, 2/4 of UGT substrates, 2/2 of FMO substrates, 1/3 of esterase substrates, 1/3 of reductase substrates, and 0/3 of AO substrates were predicted within 3-fold of observed values. In hepatocytes, CL_{int} values for 10/15 of P450 substrates, 1/4 of UGT substrates, 2/2 of FMO substrates, 3/3 of esterase substrates, 2/3 of reductase substrates, and 0/3 of AO substrates were predicted within 3-fold of observed values. Predicted CL_{int} values using metabolic stability in all systems were considerably lower than observed CL_{int} values for omeprazole and lansoprazole. For UGT substrates, diclofenac and gemfibrozil were over-predicted, whereas telmisartan was much under-predicted in microsomes and S9. In microsomes, CL_{int} values for 2/3 of esterase substrates, 1/3 of reductase substrates, and 3/3 of AO substrates were substantially under-predicted (> 10-

fold). Especially, for all of the AO substrates, predicted CL_{int} values in microsomes were extremely lower than observed CL_{int} values (> 50-fold). In S9 and hepatocytes, the predictability for mebendazole, flumazenil, rivastigmine, and all of the AO substrates was higher than that in microsomes, in spite of under-prediction for most compounds.

Prediction of Hepatic CL_{int} from Hepatocytes Corrected with Empirical Scaling Factor ("Hepatocytes + Empirical SF")

Predictability of CL_{int} values using metabolic stability in "hepatocytes + empirical SF" is shown in Tables II and Table III and Fig. 3a. CL_{int} values for 11/15 of P450 substrates, 4/4 of UGT substrates, 1/2 of FMO substrates,

Table II. $CL_{int,observed}$ Values and $CL_{int,predicted}$ Values in Human Microsomes, S9, and Hepatocytes With Or Without Scaling Factor

Compounds	$CL_{int,observed}$ (mL/min/kg)	$CL_{int,predicted}$ (mL/min/kg)					
		Microsomes	S9	Hepatocytes	Hepatocytes (SF = 3.1[e])	Hepatocytes (SF = monkey)	Hepatocytes (SF = rat)
CYP2C substrates							
Lansoprazole	4.42	0.419 ± 0.12	0.620 ± 0.17	0.324 ± 0.079	1.29	0.650	0.43
Omeprazole	21.0	1.16 ± 0.67	0.636 ± 0.26	1.13 ± 0.34	4.54	4.90	6.55
Paclitaxel	3.67	4.71 ± 5.9	4.41 ± 1.1	2.12 ± 2.7	8.48	5.30	1.38
CYP2D6 substrates							
Alprenolol	21.9	37.4 ± 4.8	31.5 ± 18	10.4 ± 0.71	41.7	11.6	–[a]
Atomoxetine	13.8	6.59 ± 0.79	3.74 ± 0.66	2.59 ± 0.83	10.3	13.2	–[a]
Desipramine	19.1	18.6 ± 2.2	26.2 ± 18	7.62 ± 0.99	30.5	13.9	29.2
Imipramine	21.3	7.00 ± 2.8	5.73 ± 3.6	25.7 ± 14	103	23.5	145
Paroxetine	13.4	57.6 ± 8.7	22.7 ± 5.3	16.3 ± 2.1	65.0	17.9	31.9
CYP3A4 substrates							
Carbamazepine	0.977	0.341 ± 0.078	0.265 ± 0.068	0.407 ± 0.39	1.63	1.65	1.26
Cisapride	6.64	2.35 ± 0.12	2.74 ± 0.87	1.37 ± 0.42	5.5	4.03	47.9
Felodipine	37.6	11.3 ± 4.4	12.4 ± 7.9	20.4 ± 12	81.8	28.0	6.57
Midazolam	14.4	11.4 ± 0.53	13.1 ± 1.3	6.67 ± 2.3	26.7	13.9	35.9
Nicardipine	31.3	69.3 ± 9.1	62.3 ± 3.9	14.0 ± 1.3	56.1	19.7	16.2
Nifedipine	21.9	11.2 ± 4.8	11.2 ± 4.5	11.4 ± 1.5	45.4	43.2	144
Nimodipine	50.3	54.6 ± 0.94	49.1 ± 1.2	11.4 ± 4.5	45.5	16.8	25.1
UGT substrates							
Diclofenac	6.81	23.3 ± 4.4	14.3 ± 1.8	1.02 ± 0.54	4.07	15.9	50.9
Gemfibrozil	3.24	44.7 ± 3.9	24.1 ± 2.9	2.74 ± 1.4	11.0	3.09	1.43
Mycophenolic acid	4.80	6.93 ± 0.80	2.68 ± 0.25	1.11 ± 2.4	4.45	6.33	1.86
Telmisartan	8.76	0.560 ± 0.11	–[c]	2.07 ± 0.55	8.29	7.23	14.7
FMO substrates							
Clozapine	3.17	4.07 ± 0.14	2.20 ± 0.78	2.31 ± 0.77	9.22	12.9	–[a]
Ranitidine	3.29	4.26 ± 1.1	4.88 ± 1.9	3.91 ± 0.98	15.7	4.96	7.67
Esterase substrates							
Flumazenil	13.9	0.847 ± 0.10	4.34 ± 1.1	4.19 ± 1.9	16.8	8.54	–[d]
Oxybutynin	7.29	5.07 ± 0.027	5.49 ± 0.33	4.77 ± 1.1	19.1	4.03	–[d]
Rivastigmine	14.1	1.41 ± 0.38	5.86 ± 1.1	8.43 ± 0.89	33.7	12.3	–[d]
Reductase substrates							
Haloperidol	6.17	7.95 ± 0.089	7.26 ± 0.74	3.13 ± 2.9	12.5	9.68	–[a]
Ketanserin	14.2	10.2 ± 0.48	3.87 ± 0.32	4.94 ± 1.9	19.7	22.0	11.3
Mebendazole	42.7	2.23 ± 0.34	4.70 ± 0.19	6.25 ± 5.8	25.0	76.5	101
AO substrates							
Zaleplon	36.3	–[b]	5.29 ± 0.69	3.35 ± 0.17	13.4	90.9	46.2
Ziprasidone	10.7	0.207 ± 0.0091	0.417 ± 0.030	1.73 ± 0.87	6.94	9.33	13.7
Zoniporide	53.0	0.973 ± 0.29	7.52 ± 1.2	3.08 ± 1.1	12.3	91.7	–[a]

N.T. not tested
Each value of $CL_{int,predicted}$ in microsomes, S9, and hepatocytes is presented as the mean ± S.D.
[a] The values could not be calculated, because CL_h in rats > Q_h (70 mL/min/kg)
[b] The values were not calculated, because the metabolic stabilities were high (the remaining ratio after incubation for 60 min with 2 mg microsomal protein/mL was > 90%)
[c] The values were not calculated, because the metabolic stabilities were high (the remaining ratio after incubation for 120 min with 4 mg S9 protein/mL was > 90%)
[d] The values were not calculated, because the compounds were metabolized in rat plasma
[e] Empirical scaling factor

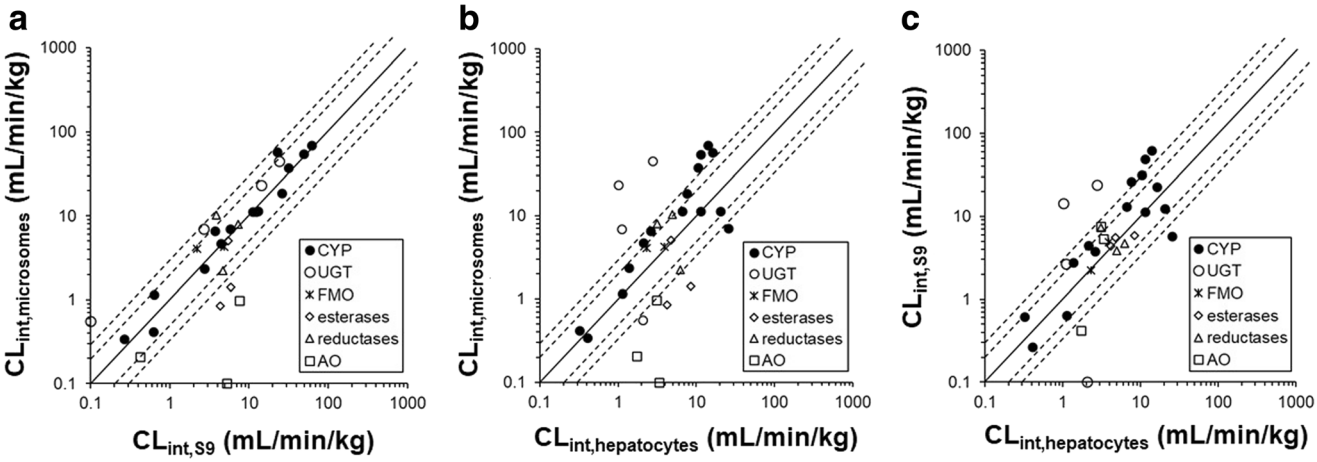

Fig. 1. Correlation among predicted CL_{int} values using metabolic stability in human microsomes, S9, and hepatocytes. Panel **a** represents the correlation between microsomes and S9. Panel **b** represents the correlation between microsomes and hepatocytes. Panel **c** represents the correlation between S9 and hepatocytes. When the metabolic stabilities were high, CL_{int} values were not calculated and were plotted as 0.1

3/3 of esterase substrates, 3/3 of reductase substrates, and 1/3 of AO substrates were predicted within 3-fold of observed values. The predictability in human hepatocytes was improved by using the empirical scaling factor.

Prediction of Hepatic CL_{int} from Hepatocytes Corrected with Monkey Scaling Factor ("Hepatocytes + Monkey SF")

Predictability of CL_{int} values using metabolic stability in "hepatocytes + monkey SF" is shown in Tables II and III and Fig. 3b. CL_{int} values for 13/15 of P450 substrates, 4/4 of UGT substrates, 1/2 of FMO substrates, 3/3 of esterase substrates, 3/3 of reductase substrates, and 3/3 of AO substrates were predicted within 3-fold of observed values. The predictability in human hepatocytes was considerably improved by using monkey scaling factor, and this method showed the highest predictability among the six methods investigated for substrates of all enzymes except for FMO.

Prediction of CL_{int} from Hepatocytes Corrected with Rat Scaling Factor ("Hepatocytes + Rat SF")

Predictability of CL_{int} values using metabolic stability in "hepatocytes + rat SF" is shown in Tables II and III and Fig. 3c. CL_{int} values for 7/13 of P450 substrates, 3/4 of UGT substrates, 1/1 of FMO substrates, 2/2 of reductase substrates and 2/2 of AO substrates were predicted within 3-fold of observed values. The predictability in human hepatocytes was improved by using rat scaling factor for substrates of UGT, reductases, and AO.

Comparison of Predictability of CL_{int} Among the Methods Investigated in This Study

Predictability of CL_{int} values by six methods for 30 compounds (22 compounds for the method using "hepatocytes + rat SF") is shown in Table IV and Figs. 2 and 3. CL_{int} values for 50% (15/30) compounds in microsomes, 50% (15/30) compounds in S9, 60% (18/30) compounds in hepatocytes, 77% (23/30) compounds in "hepatocytes + empirical SF," 90% (27/30) compounds in "hepatocytes + monkey SF," and 68% (15/22) compounds in "hepatocytes + rat SF" were predicted within 3-fold of observed values. In addition, the AFE value of "hepatocytes + monkey SF" method (AFE = 1.72) was the least among the six methods. Therefore, the "hepatocytes + monkey SF" method showed the best predictability.

DISCUSSION

In the current study, predictability of the prediction methods using microsomes, S9, cryopreserved hepatocytes with or without scaling factor for substrates of P450, UGT, FMO, esterases, reductases, and AO was evaluated.

For P450 substrates, microsomes and S9 showed comparable predictability of CL_{int} values. This result suggests that S9 can be used instead of microsomes for estimating hepatic clearance. The CL_{int} values of desipramine, felodipine, imipramine, midazolam, nifedipine, and omeprazole in microsomes were similar to those previously reported (27). Predicted CL_{int} values in hepatocytes for most compounds were underestimated compared to observed values (Fig. 2c). This result is consistent with a previous report (15). In all three systems, the predicted CL_{int} values were considerably lower than observed values for CYP2C19 substrates, omeprazole, and lansoprazole. It is necessary to investigate whether the considerable under-estimation is common to CYP2C19 substrates. The "hepatocytes + monkey SF" method showed comparable prediction accuracy to the reported method using microsomes with rat or dog scaling factors (17).

Glucuronidation, via UGT in microsomes, is an important clearance mechanism for many drugs (28,29). Kilford *et al.* reported that addition of 2% BSA improved the predictability in microsomes, and the combined cofactor of NADPH and UDPGA was applicable for compounds that are metabolized by both P450 and UGT (20). The incubation conditions of their report were applied to UGT substrates in the current study. The CL_{int} value of diclofenac, substrate of UGT1A9, UGT2B7, and CYP2C9, was consistent with the value reported by them, and they reported that predictability of midazolam (CYP3A4 substrate) was high (20,29,30).

Table III. Predictability of CL_{int} Values for Substrates of P450, UGT, Reductases, AO, FMO, and Esterases in Human Microsomes, S9, and Hepatocytes With Or Without Scaling Factor

	Number of drugs/total drugs					
	Microsomes	S9	Hepatocytes	Hepatocytes (SF = 3.1[a])	Hepatocytes (SF = monkey)	Hepatocytes (SF = rat)
P450 substrates						
Within 2-fold	6/15	8/15	5/15	11/15	12/15	4/13
Within 3-fold	10/15	9/15	10/15	11/15	13/15	7/13
Within 5-fold	13/15	1 3 / 15	12/15	14/15	14/15	8/13
UGT substrates						
Within 2-fold	1/4	1/4	1/4	2/4	3/4	1/4
Within 3-fold	1/4	2/4	1/4	4/4	4/4	3/4
Within 5-fold	2/4	2/4	3/4			3/4
FMO substrates						
Within 2-fold	2/2	2/2	2/2	0/2	1/2	0/1
Within 3-fold				1/2	1/2	1/1
Within 5-fold				2/2	2/2	
Esterases substrates						
Within 2-fold	0/3	1/3	2/3	2/3	3/3	
Within 3-fold	0/3	1/3	3/3	3/3		
Within 5-fold	0/3	3/3				
Reductases substrates						
Within 2-fold	2/3	1/3	1/3	2/3	3/3	1/2
Within 3-fold	2/3	1/3	2/3	3/3		2/2
Within 5-fold	2/3	2/3	2/3			
AO substrates						
Within 2-fold	0/3	0/3	0/3	1/3	2/3	2/2
Within 3-fold	0/3	0/3	0/3	1/3	3/3	
Within 5-fold	0/3	0/3	0/3	2/3		

[a] Empirical scaling factor

Therefore, the incubation conditions seem to be applicable to P450 substrates and UGT substrates. Gemfibrozil, mycophenolic acid, and telmisartan are predominantly metabolized by UGT2B7, UGT1A9, and UGT1A3, respectively (29,31,32). The results for gemfibrozil (over-prediction) and telmisartan (under-prediction) in microsomes were similar to those in a previous report (29). The trend of over- and under-prediction was also observed in S9. Similar with P450 substrates, predicted CL_{int} values in hepatocytes were underestimated compared to observed values regardless of UGT isoforms.

FMO is a major mammalian non-P450 oxidative enzyme in microsomes. The major isoform in the adult human liver is FMO3 (33). Clozapine and ranitidine are mainly metabolized by FMO3 in humans (2,34). Predictability of CL_{int} values for these compounds was very high in microsomes, S9, and hepatocytes, without a scaling factor.

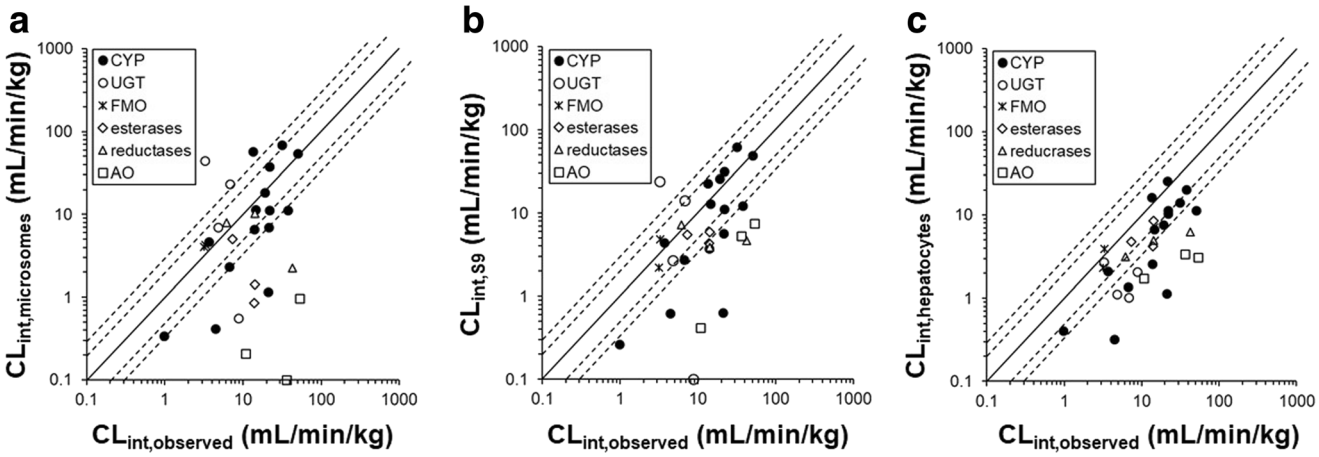

Fig. 2. Correlation between predicted CL_{int} values and observed CL_{int} values in human microsomes, S9, and hepatocytes. Panels **a**–**c** represent the correlation in microsomes, S9, and hepatocytes, respectively. When the metabolic stabilities were high, CL_{int} values were not calculated and were plotted as 0.1

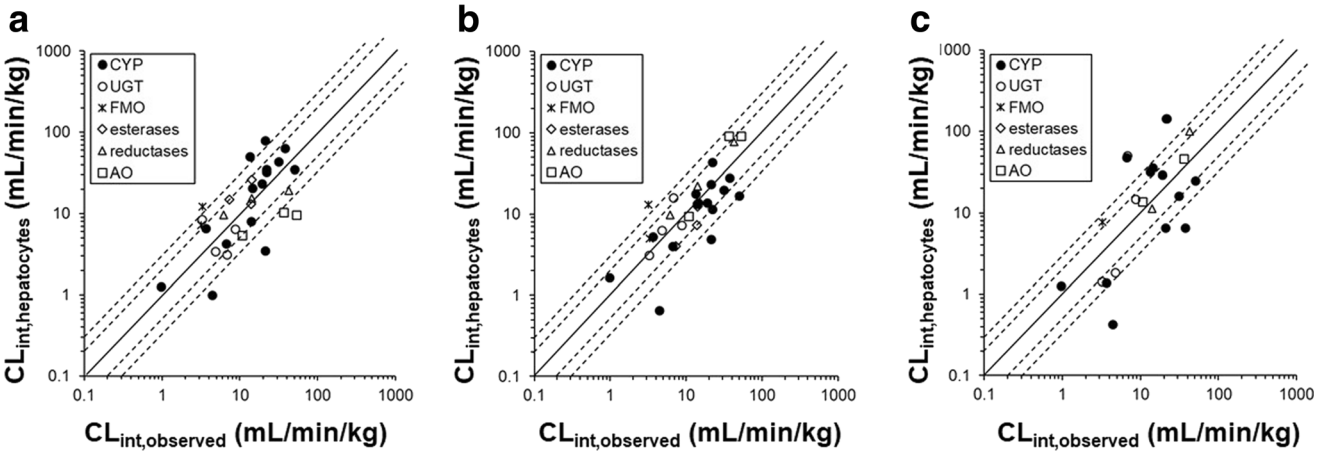

Fig. 3. Correlation between predicted CL_{int} values and observed CL_{int} values in hepatocytes corrected with empirical, monkey, and rat scaling factors. Panels **a**–**c** represent the correlation in hepatocytes corrected with empirical, monkey, and rat scaling factors, respectively

The contribution of esterases to clearance for the top 200 drugs in 2002 was the third largest after P450 and UGT (35). Esterases hydrolyze the compounds that contain ester, amide, and thioester bonds. Among esterases, carboxylesterases (CES) are well-known to be involved in the hydrolysis of various drugs (36). Flumazenil is primarily metabolized by hepatic CES, although the isoform is unknown (37). Oxybutynin is mainly metabolized by CES1 and CYP3A4 (38,39). Rivastigmine is metabolized by esterases, although the enzyme is unknown (40). Predicted CL_{int} values in microsomes for flumazenil and rivastigmine were considerably underestimated compared with observed values, and the predictabilities of CL_{int} values in S9 and hepatocytes were higher than those in microsomes. This might be because CES is expressed not only in the endoplasmic reticulum but also in cytosol (41).

Prediction methods of hepatic clearance for a number of substrates of reductive enzymes have not been reported. Most carbonyl-reducing drug enzymes are divided into aldo-keto reductase (AKR), carbonyl reductase (CBR), and 11β-hydroxysteroid dehydrogenase (11β-HSD) (42–44). These enzymes are NADPH and/or NADH-dependent, and AKR and CBR are cytosolic enzymes and 11β-HSD is a microsomal enzyme (45). Major metabolic enzymes of haloperidol were CBR, CYP3A4, and UGT (46). Major metabolic routes of mebendazole were reduction by CBR in cytosol and hydrolysis in microsomes (47,48). The reductive enzyme of ketanserin is unclear, but it was suggested that it was metabolized by 11β-HSD (49,50). Even in S9 and hepatocytes, predicted CL_{int} values for mebendazole were lower than observed CL_{int} values. The prediction method of "hepatocytes + monkey SF" would be useful for compounds like mebendazole.

Recently, the reports about drugs that are mainly metabolized by AO have increased (51). AO is a cofactor-independent cytosolic enzyme (52). Ziprasidone is metabolized by AO and CYP3A4 (53,54). Zaleplon and zoniporide are metabolized mainly by AO (55,56). As suggested from the localization, CL_{int} values in microsomes were lower than those in S9 and hepatocytes for all of three AO substrates. However, even in S9 and hepatocytes, predicted CL_{int} values were considerably lower than observed CL_{int} values. It was reported that predicted CL_{int} using S9 and hepatocytes for AO substrates were underestimated by around 10-fold (56,57). Similar results were observed in the present study. The predictability in human hepatocytes was improved by using monkey and rat scaling factors.

Predictability of CL_{int} values in human hepatocytes was improved by using an empirical scaling factor. The empirical scaling factor in the current study was 3.1-fold. Shibata *et al.* also reported empirical scaling factors of approximately 3- to 4-fold determined by a "serum incubation method" (15). However, the CL_{int} values of imipramine (CL_{int} in the present study *vs* report = 11 *vs* 1.78 μL/min/10^6 cells) and diclofenac (0.25 *vs* 0.77 μL/min/10^6 cells) showed 6-fold and 3-fold difference from the values of their report, respectively (15).

Table IV. Predictability of CL_{int} Values in Human Microsomes, S9, and Hepatocytes With Or Without Scaling Factor

	Number of drugs/total drugs					
	Microsomes	S9	Hepatocytes	Hepatocytes (SF = 3.1[a])	Hepatocytes (SF = monkey)	Hepatocytes (SF = rat)
Within 2-fold	11/30	13/30	11/30	18/30	24/30	8/22
Within 3-fold	15/30	15/30	18/30	23/30	27/30	15/22
Within 5-fold	19/30	22/30	22/30	28/30	29/30	16/22
AFE	4.98	3.36	3.20	2.03	1.72	2.79

For the prediction method using microsomes data, the CL_{int} value for zaleplon was assumed as 0.1 mL/min/kg. For the prediction method using S9 data, the CL_{int} value for telmisartan was assumed as 0.1 mL/min/kg. For the prediction method using human hepatocytes data with scaling factor of rat, 23 compounds other than alprenolol, atomoxetine, haloperidol, zoniporide, clozapine, flumazenil, and oxybutynin were estimated
[a] Empirical scaling factor

The hepatocytes in the present study and in the report were pooled from 20 and 2 donors, respectively.

Predictability of CL_{int} values in human hepatocytes was improved by either monkey or rat scaling factor. However, the degree of improvement by the "hepatocytes + monkey SF" method was considerably higher than that by the "hepatocytes + rat SF" method. Furthermore, the "hepatocytes + monkey SF" method showed higher predictability than the "hepatocytes + empirical SF" method (Table IV). This result suggests that the *in vitro-in vivo* correlation (IVIVC) for each compound is similar between humans and monkeys. It was hypothesized that hepatocytes do not retain metabolic activities of all enzymes and the degree of decrease in metabolic activity differs among enzymes. On the other hand, no apparent correlation between scaling factors of rats and humans for hepatocytes or microsomes have been reported (27). In addition, *in vivo* rat CL_h values of a number of compounds were higher than liver blood flow rate (Table II). Many of these compounds were non-P450 substrates; therefore, there is a possibility that one of the reasons for the high CL_h in rats is extra-hepatic metabolism by non-P450 enzymes. For compounds for which the observed human or monkey R_b values were not reported, we assumed that human R_b = rat R_b and monkey R_b = human or rat R_b (Supplemental Table 4). Uchimura *et al.* reported that assuming human R_b = rat R_b was more accurate than assuming human $R_b = 1$ (58). In addition, in the present study, the reported monkey R_b values were not extremely different from human or rat R_b values, although available data were limited. The $f_{u,p}$ values of monkeys and rats were measured in the present study, whereas reported human $f_{u,p}$ data was used (Supplemental Table 4).

The focus of the present study was on drug metabolizing enzymes. As such, the majority of the compounds investigated were not substrates of transporters, which could confound the IVIVC. It has reported that the prediction of hepatic clearance for substrates of transporters using hepatocytes showed higher predictability compared with that using subcellular fractions (59,60). Furthermore, Izumi *et al.* reported that the prediction using only hepatic uptake clearance showed higher prediction accuracy than that using metabolic clearance and uptake clearance in hepatocytes (60). It is necessary to focus on metabolism/transporter interplay in future study.

In the drug discovery stage, the enzymes responsible for the metabolism of new chemical entities are unknown and there is a possibility that multiple enzymes that are localized in different fractions are involved in the metabolism. Hepatocytes can be used to estimate various kinds of compounds, regardless of cofactors and localization of metabolic enzymes. There was little difference in the predictability between compounds that are cleared by a single enzyme and those cleared by multiple enzymes, not only in hepatocytes but also in subcellular fractions. This may be due to the addition of NADPH to the incubations of subcellular fractions for all compounds, including non-P450 substrates. Further study using more compounds that are cleared by multiple enzymes other than P450 is needed. Furthermore, the "serum incubation method" can be applied to hepatocytes, which is a simple method with no need to add cofactors, know the localization of metabolic enzymes involved, or determine protein binding, and the predictability of CL_{int} values using the prediction method of "hepatocytes + monkey SF" with "serum incubation method" for various compounds, including non-P450 substrates, was the highest in this study (Table IV). Therefore, this method will be very useful for new chemical entities from the drug discovery stage to the pre-clinical stage.

CONCLUSION

The prediction using human hepatocytes corrected with monkey scaling factor showed the highest predictability for both P450 and non-P450 substrates among the predictions using microsomes, S9, and hepatocytes with or without scaling factors. This method is accurate and useful for estimating new chemical entities with no need to care about cofactors, localization of metabolic enzymes, or protein binding in plasma and incubation mixture.

REFERENCES

1. Obach RS. The prediction of human clearance from hepatic microsomal metabolism data. Curr Opin Drug Discov Dev 2013. 2001;4:36–44.
2. Chung WG, Park CS, Roh HK, Lee WK, Cha YN. Oxidation of ranitidine by isozymes of flavin-containing monooxygenase and cytochrome P450. Jpn J Pharmacol. 2000;84:213–20.
3. Wienkers LC, Heath TG. Predicting in vivo drug interactions from in vitro drug discovery data. Nat Rev Drug Discov. 2005;4:825–33.
4. Mordenti J. Pharmacokinetic scale-up: accurate prediction of human pharmacokinetic profiles from animal data. J Pharm Sci. 1985;74:1097–9.
5. Ings RM. Interspecies scaling and comparisons in drug development and toxicokinetics. Xenobiotica. 1990;20:1201–31.
6. Lavé T, Coassolo P, Reigner B. Prediction of hepatic metabolic clearance based on interspecies allometric scaling techniques and in vitro-in vivo correlations. Clin Pharmacokinet. 1999;36:211–31.
7. Houston JB. Utility of in vitro drug metabolism data in predicting in vivo metabolic clearance. Biochem Pharmacol. 1994;47:1469–79.
8. Iwatsubo T, Hirota N, Ooie T, Suzuki H, Shimada N, Chiba K, et al. Prediction of in vivo drug metabolism in the human liver from in vitro metabolism data. Pharmacol Ther. 1997;73:147–71.
9. Hallifax D, Houston JB. Methodological uncertainty in quantitative prediction of human hepatic clearance from in vitro experimental systems. Curr Drug Metab. 2009;10:307–21.
10. Kola I, Landis J. Can the pharmaceutical industry reduce attrition rates? Nat Rev Drug Discov. 2004;3:711–5.
11. Margolis JM, Obach RS. Impact of nonspecific binding to microsomes and phospholipid on the inhibition of cytochrome P4502D6: implications for relating in vitro inhibition data to in vivo drug interactions. Drug Metab Dispos. 2003;31:606–11.
12. Chiba M, Ishii Y, Sugiyama Y. Prediction of hepatic clearance in human from in vitro data for successful drug development. AAPS J. 2009;11:262–76.
13. Riccardi K, Cawley S, Yates PD, Chang C, Funk C, Niosi M, et al. Plasma protein binding of challenging compounds. J Pharm Sci. 2015;104:2627–36.

14. Shibata Y, Takahashi H, Ishii Y. A convenient in vitro screening method for predicting in vivo drug metabolic clearance using isolated hepatocytes suspended in serum. Drug Metab Dispos. 2000;28:1518–23.
15. Shibata Y, Takahashi H, Chiba M, Ishii Y. Prediction of hepatic clearance and availability by cryopreserved human hepatocytes: an application of serum incubation method. Drug Metab Dispos. 2002;30:892–6.
16. Shibata Y, Kuze J, Chiba M. Utility of cryopreserved hepatocytes suspended in serum to predict hepatic clearance in dogs and monkeys. Drug Metab Pharmacokinet. 2014;29:168–76.
17. Naritomi Y, Terashita S, Kimura S, Suzuki A, Kagayama A, Sugiyama Y. Prediction of human hepatic clearance from in vivo animal experiments and in vitro metabolic studies with liver microsomes from animals and humans. Drug Metab Dispos. 2001;29:1316–24.
18. Naritomi Y, Terashita S, Kagayama A, Sugiyama Y. Utility of hepatocytes in predicting drug metabolism: comparison of hepatic intrinsic clearance in rats and humans in vivo and in vitro. Drug Metab Dispos. 2003;31:580–8.
19. Fisher MB, Campanale K, Ackermann BL, VandenBranden M, Wrighton SA. In vitro glucuronidation using human liver microsomes and the pore-forming peptide alamethicin. Drug Metab Dispos. 2000;28:560–6.
20. Kilford PJ, Stringer R, Sohal B, Houston JB, Galetin A. Prediction of drug clearance by glucuronidation from in vitro data: use of combined cytochrome P450 and UDP-glucuronosyltransferase cofactors in alamethicin-activated human liver microsomes. Drug Metab Dispos. 2009;37:82–9.
21. Zhang Y, Yao L, Lin J, Gao H, Wilson TC, Giragossian C. Lack of appreciable species differences in nonspecific microsomal binding. J Pharm Sci. 2010;99:3620–7.
22. Langmuir I. The adsorption of gases on plane surfaces of glass, mica and platinum. J Am Chem Soc. 1918;40:1361–403.
23. Hosea NA, Collard WT, Cole S, Maurer TS, Fang RX, Jones H, et al. Prediction of human pharmacokinetics from preclinical information: comparative accuracy of quantitative prediction approaches. J Clin Pharmacol. 2009;49:513–33.
24. Houston JB, Galetin A. Methods for predicting in vivo pharmacokinetics using data from in vitro assays. Curr Drug Metab. 2008;9:940–51.
25. Roberts MS, Rowland M. Correlation between in-vitro microsomal enzyme activity and whole organ hepatic elimination kinetics; analysis with a dispersion model. J Pharm Pharmacol. 1986;38:177–81.
26. Obach RS, Baxter JG, Liston TE, Silber BM, Jones BC, MacIntyre F, et al. The prediction of human pharmacokinetic parameters from preclinical and in vitro metabolism data. J Pharmacol Exp Ther. 1997;283:46–58.
27. Wood FL, Houston JB, Hallifax D. Clearance prediction methodology needs fundamental improvement: trends common to rat and human hepatocytes/microsomes and implications for experimental methodology. Drug Metab Dispos. 2017;45:1178–88.
28. Kiang TK, Ensom MH, Chang TK. UDP-glucuronosyltransferases and clinical drug-drug interactions. Pharmacol Ther. 2005;106:97–132.
29. Gill KL, Houston JB, Galetin A. Characterization of in vitro glucuronidation clearance of a range of drugs in human kidney microsomes: comparison with liver and intestinal glucuronidation and impact of albumin. Drug Metab Dispos. 2012;40:825–35.
30. King C, Tang W, Ngui J, Tephly T, Braun M. Characterization of rat and human UDP-glucuronosyltransferases responsible for the in vitro glucuronidation of diclofenac. Toxicol Sci. 2001;61:49–53.
31. Mano Y, Usui T, Kamimura H. The UDP-glucuronosyltransferase 2B7 isozyme is responsible for gemfibrozil glucuronidation in the human liver. Drug Metab Dispos. 2007;35:2040–4.
32. Yamada A, Maeda K, Ishiguro N, Tsuda Y, Igarashi T, Ebner T, et al. The impact of pharmacogenetics of metabolic enzymes and transporters on the pharmacokinetics of telmisartan in healthy volunteers. Pharmacogenet Genomics. 2011;21:523–30.
33. Overby LH, Carver GC, Philpot RM. Quantitation and kinetic properties of hepatic microsomal and recombinant flavin-containing monooxygenases 3 and 5 from humans. Chem Biol Interact. 1997;106:29–45.
34. Tugnait M, Hawes EM, McKay G, Rettie AE, Haining RL, Midha KK. N-oxygenation of clozapine by flavin-containing monooxygenase. Drug Metab Dispos. 1997;25:524–7.
35. Williams JA, Hyland R, Jones BC, Smith DA, Hurst S, Goosen TC, et al. Drug-drug interactions for UDP-glucuronosyltransferase substrates: a pharmacokinetic explanation for typically observed low exposure (AUCi/AUC) ratios. Drug Metab Dispos. 2004;32:1201–8.
36. Fukami T, Yokoi T. The emerging role of human esterases. Drug Metab Pharmacokinet. 2012;27:466–77.
37. Franssen EJF, Greuter HNJM, Touw DJ, Luurtsema G, Windhorst AD, Lammertsma AA. Plasma pharmacokinetics of [^{11}C]-flumazenil and its major metabolite [^{11}C]-flumazenil 'acid'. Br J Clin Pharmacol. 2002;53:554Pb.
38. Lukkari E, Taavitsainen P, Juhakoski A, Pelkonen O. Cytochrome P450 specificity of metabolism and interactions of oxybutynin in human liver microsomes. Pharmacol Toxicol. 1998;82:161–6.
39. Sato Y, Miyashita A, Iwatsubo T, Usui T. Conclusive identification of the oxybutynin-hydrolyzing enzyme in human liver. Drug Metab Dispos. 2012;40:902–6.
40. Noetzli M, Eap CB. Pharmacodynamic, pharmacokinetic and pharmacogenetic aspects of drugs used in the treatment of Alzheimer's disease. Clin Pharmacokinet. 2013;52:225–41.
41. Satoh T, Hosokawa M. The mammalian carboxylesterases: from molecules to functions. Annu Rev Pharmacol Toxicol. 1998;38:257–88.
42. Maser E. Xenobiotic carbonyl reduction and physiological steroid oxidoreduction. The pluripotency of several hydroxysteroid dehydrogenases. Biochem Pharmacol. 1995;49:421–40.
43. Oppermann UC, Maser E. Molecular and structural aspects of xenobiotic carbonyl metabolizing enzymes. Role of reductases and dehydrogenases in xenobiotic phase I reactions. Toxicology. 2000;144:71–81.
44. Parkinson A. An overview of current cytochrome P450 technology for assessing the safety and efficacy of new materials. Toxicol Pathol. 1996;24:48–57.
45. Rosemond MJ, Walsh JS. Human carbonyl reduction pathways and a strategy for their study in vitro. Drug Metab Rev. 2004;36:335–61.
46. Kudo S, Ishizaki T. Pharmacokinetics of haloperidol: an update. Clin Pharmacokinet. 1999;37:435–56.
47. Dawson M, Braithwaite PA, Roberts MS, Watson TR. The pharmacokinetics and bioavailability of a tracer dose of [3H]-mebendazole in man. Br J Clin Pharmacol. 1985;19:79–86.
48. Nishimuta H, Nakagawa T, Nomura N, Yabuki M. Significance of reductive metabolism in human intestine and quantitative prediction of intestinal first-pass metabolism by cytosolic reductive enzymes. Drug Metab Dispos. 2013;41:1104–11.
49. Persson B, Heykants J, Hedner T. Clinical pharmacokinetics of ketanserin. Clin Pharmacokinet. 1991;20:263–79.
50. Mazur CS, Kenneke JF, Goldsmith MR, Brown C. Contrasting influence of NADPH and a NADPH-regenerating system on the metabolism of carbonyl-containing compounds in hepatic microsomes. Drug Metab Dispos. 2009;37:1801–5.
51. Pryde DC, Dalvie D, Hu Q, Jones P, Obach RS, Tran TD. Aldehyde oxidase: an enzyme of emerging importance in drug discovery. J Med Chem. 2010;53:8441–60.
52. Jones JP, Korzekwa KR. Predicting intrinsic clearance for drugs and drug candidates metabolized by aldehyde oxidase. Mol Pharm. 2013;10:1262–8.
53. Beedham C, Miceli JJ, Obach RS. Ziprasidone metabolism, aldehyde oxidase, and clinical implications. J Clin Psychopharmacol. 2003;23:229–32.
54. Miao Z, Kamel A, Prakash C. Characterization of a novel metabolite intermediate of ziprasidone in hepatic cytosolic fractions of rat, dog, and human by ESI-MS/MS, hydrogen/deuterium exchange, and chemical derivatization. Drug Metab Dispos. 2005;33:879–83.
55. Lake BG, Ball SE, Kao J, Renwick AB, Price RJ, Scatina JA. Metabolism of zaleplon by human liver: evidence for involvement of aldehyde oxidase. Xenobiotica. 2002;32:835–47.

56. Zientek M, Jiang Y, Youdim K, Obach RS. In vitro-in vivo correlation for intrinsic clearance for drugs metabolized by human aldehyde oxidase. Drug Metab Dispos. 2010;38:1322–7.
57. Akabane T, Gerst N, Masters JN, Tamura K. A quantitative approach to hepatic clearance prediction of metabolism by aldehyde oxidase using custom pooled hepatocytes. Xenobiotica. 2012;42:863–71.
58. Uchimura T, Kato M, Saito T, Kinoshita H. Prediction of human blood-to-plasma drug concentration ratio. Biopharm Drug Dispos. 2010;31:286–97.
59. Watanabe T, Kusuhara H, Maeda K, Kanamaru H, Saito Y, Hu Z, et al. Investigation of the rate-determining process in the hepatic elimination of HMG-CoA reductase inhibitors in rats and humans. Drug Metab Dispos. 2010;38:215–22.
60. Izumi S, Nozaki Y, Komori T, Takenaka O, Maeda K, Kusuhara H, et al. Comparison of the predictability of human hepatic clearance for organic anion transporting polypeptide substrate drugs between different in vitro-in vivo extrapolation approaches. J Pharm Sci. 2017;106:2678–87.